Associated Production of Light Gravitinos at Future Linear Colliders

Kentarou Mawatari [*]

Theoretische Natuurkunde and IIHE/ELEM, Vrije Universiteit Brussel,
and International Solvay Institutes, Pleinlaan 2, B-1050 Brussels, Belgium

We study light gravitino productions in association with a neutralino at future linear colliders in a scenario in which the lightest SUSY particle is a gravitino and the produced neutralino promptly decays into a photon and a gravitino. Comparing with the multiple goldstino scenario, we show that energy and angular distributions of the photon provide valuable information on the SUSY masses as well as the SUSY breaking.

1 Introduction

Gravitino productions in association with a SUSY particle are known processes which become significant at colliders when the gravitino is very light as $m_{3/2} \sim \mathcal{O}(10^{-2}$ eV$)$ or less, since the cross sections are inversely proportional to the square of the Planck scale times the gravitino mass

$$\sigma \propto 1/(M_{\mathrm{Pl}} m_{3/2})^2. \tag{1}$$

When the associated SUSY particle is the next-to-lightest SUSY particle (NLSP) and promptly decays into a SM particle and a LSP gravitino, the production processes lead to particular collider signatures, e.g. $\gamma + \not{E}$ and $j + \not{E}$, where the missing energy is carried away by two gravitinos, and these signals set mass bounds on the gravitino and the other SUSY particles. It should be noted that the gravitino mass is related to the SUSY breaking scale as well as the Planck scale like

$$m_{3/2} \sim (M_{\mathrm{SUSY}})^2/M_{\mathrm{Pl}}. \tag{2}$$

The current experimental bound on the gravitino mass from the single-photon plus missing-energy signal in neutralino-gravitino associated productions is given by the LEP experiment as a function of the neutralino and selectron masses, e.g.

$$m_{3/2} \gtrsim 10^{-5} \text{ eV, i.e. } M_{\mathrm{SUSY}} \gtrsim 200 \text{ GeV}, \tag{3}$$

for $m_{\tilde{\chi}_1^0} = 140$ GeV and $m_{\tilde{e}} = 150$ GeV [1].

Several theoretical studies on the $\tilde{\chi}_1^0$-$\tilde{G}$ productions in e^+e^- collisions had been done before especially for the LEP [2–4], and recently the process was restudied for future linear colliders with the then current simulation tools [5,6] in Ref. [7]. We note that such a very light gravitino is suggested by the context of no-scale supergravity [8,9] and some extra-dimensional models [10], while in typical gauge-mediated SUSY breaking (GMSB) scenarios we expect a mass of 1 eV–10 keV [11].

In this report, we extend our previous study on the process $e^+e^- \to \tilde{\chi}_1^0 \tilde{G}$ [7] with the latest tools, `FeynRules` [12,13] and `MadGraph5` [14], and make a comparison with the multiple goldstino scenario, which was presented recently in Ref. [15].
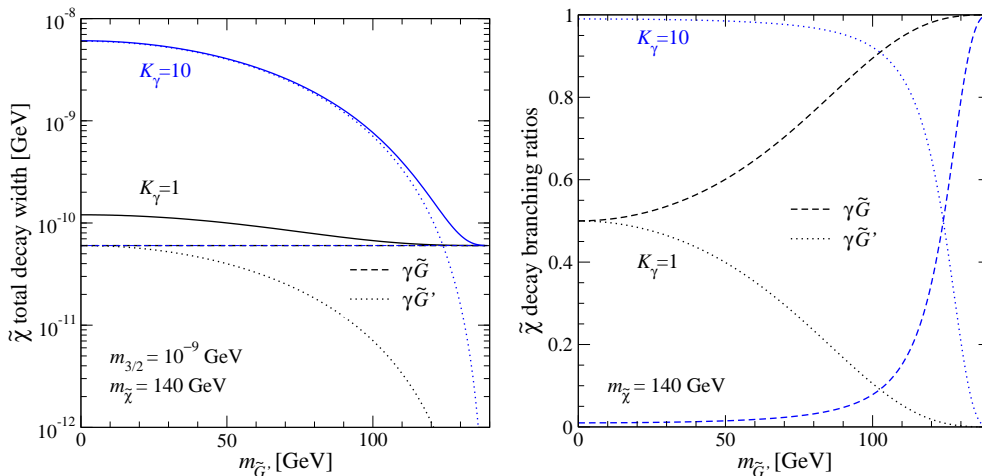

1

Figure 1: Total decay width (left) and decay branching ratios (right) of the lightest neutralino, assumed as a pure photino, as a function of the pseudo-goldstino mass for $K_\gamma = 1$ (black lines) and 10 (blue lines).

2   Goldstini in gauge mediation

Multiple goldstino models, so-called *goldstini* models [16], in the framework of gauge mediation are characterized by a visible sector (e.g. the MSSM) coupled by gauge interactions to more than one SUSY breaking sector [17]. The spectrum consists of a light gravitino LSP, behaving as a goldstino, and a number of neutral fermions (the pseudo-goldstini) with a mass between that of the LSP and that of the lightest observable-sector SUSY particle (LOSP). Here we consider a situation where the LOSP is the lightest neutralino and there is only one pseudo-goldstino with a mass of $\mathcal{O}(100)$ GeV. The coupling of the MSSM particles to the pseudo-goldstino can be enhanced with respect to those of the gravitino giving rise to characteristic signatures. The relevant pseudo-goldstino interaction Lagrangian is shown in Appendix A.

To highlight the differences with respect to the case of the single SUSY breaking sector and the role played by the extra parameters K, characterizing the pseudo-goldstino couplings, we present the total decay width and the decay branching ratios of the lightest neutralino in Fig. 1. For simplicity we assume the neutralino is a pure photino in this report. The partial decay width for the decay into a photon and a pseudo-goldstino is given by [15]

$$\Gamma(\tilde{\chi}_1^0 \rightarrow \gamma\tilde{G}') = \frac{K_\gamma^2 |C_{\gamma\tilde{\chi}_1}|^2 m_{\tilde{\chi}_1^0}^5}{48\pi \overline{M}_{\mathrm{Pl}}^2 m_{3/2}^2} \left(1 - \frac{m_{\tilde{G}'}^2}{m_{\tilde{\chi}_1^0}^2}\right)^3 \tag{4}$$

with the reduced Planck mass $\overline{M}_{\mathrm{Pl}} \equiv M_{\mathrm{Pl}}/\sqrt{8\pi} \sim 2.4 \times 10^{18}$ GeV and the mass of the gravitino (i.e. the true goldstino) $m_{3/2}$. $C_{\gamma\tilde{\chi}_1}$ is defined in Appendix A and equal to unity for the photino case. The $m_{\tilde{G}'} = 0$ limit with $K_\gamma = 1$ reduces (4) to $\Gamma(\tilde{\chi}_1^0 \rightarrow \gamma\tilde{G})$. The decay width and the branching ratios strongly depend on the pseudo-goldstino mass and the K_γ factor. We refer to [15] for more details and the $\tilde{\chi}_1^0 \rightarrow Z\tilde{G}'$ decay.
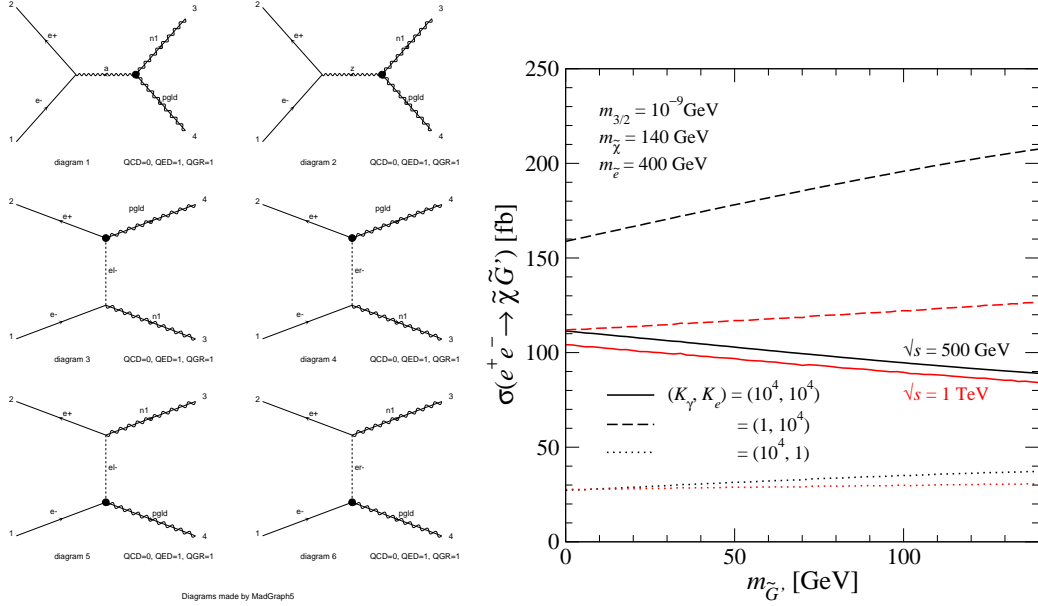
Figure 2: (Left) Feynman diagrams for the process $e^+e^- \rightarrow \tilde{\chi}_1^0\tilde{G}'$, generated by `MadGraph5` [14]. (Right) The total cross sections at $\sqrt{s} = 500$ GeV (black lines) and 1 TeV (red lines) as a function of the pseudo-goldstino mass, for various values of K_γ and K_e.

3 Single-photon plus missing energy signal

As mentioned before, in typical GMSB models, the gravitino mass is not accessible in colliders since the associated production cross section is too small. In the case of the pseudo-goldstino, however, the cross section can be enhanced by the coupling factors K while keeping the gravitino mass as $m_{3/2} \sim$ eV, i.e. $M_{\text{SUSY}} \sim 100$ TeV.

In this report, we consider pseudo-goldstino productions in association with a neutralino in e^+e^- collisions, where the produced LOSP neutralino subsequently decays into a photon and a (almost massless) gravitino or into a photon and a (massive) pseudo-goldstino,

$$e^+e^- \rightarrow \tilde{\chi}_1^0\tilde{G}'; \quad \tilde{\chi}_1^0 \rightarrow \gamma\tilde{G} \text{ or } \gamma\tilde{G}'. \tag{5}$$

The decay fraction is determined by $m_{\tilde{G}'}$ and K_γ as one can see in Fig. 1. Feynman diagrams for the production process are shown in Fig. 2 (left). Since the neutralino is assumed here to be a pure photino, we can neglect the diagram 2. In the t- and u-channels the intermediate particle is either the left- or right-handed selectron, and we assume that the coupling factor K_e is the same for both selectrons; see also the interaction Lagrangian in Appendix A. All the helicity amplitudes for the production process are presented in the $m_{\tilde{G}'} = 0$ limit in [7], while the spin summed amplitude squared is shown in [15].

Figure 2 (right) shows the production cross sections as a function of the pseudo-goldstino mass for some values of the parameters K_γ and K_e. Here we take the masses as $m_{3/2} = 10^{-9}$ GeV, $m_{\tilde{\chi}_1^0} = 140$ GeV and $m_{\tilde{e}_L} = m_{\tilde{e}_R} = 400$ GeV, while those masses as well as beam
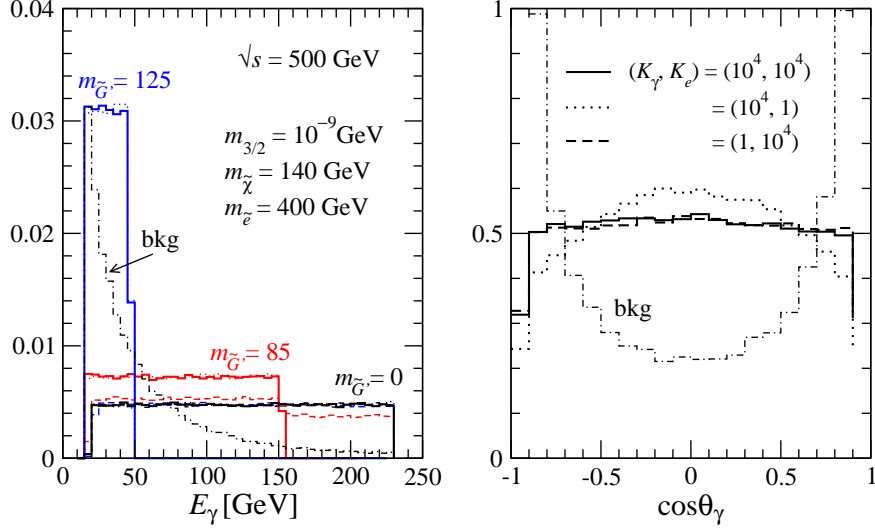
Figure 3: Normalized energy (left) and angular (right) distributions of the photon for $e^+e^- \to \tilde{\chi}_1^0 \tilde{G}' \to \gamma \tilde{G}^{(')} \tilde{G}'$ at $\sqrt{s} = 500$ GeV.

polarizations can change the cross section [7]. It should be stressed that the cross section scales with $K_{\gamma,e}^2/m_{3/2}^2$, and hence the cross section in the $m_{\tilde{G}'} = 0$ limit for $m_{3/2} = 10^{-9}$ GeV with $K_\gamma = K_e = 10^4$ is equal to that for $m_{3/2} = 10^{-13}$ GeV in the single sector scenario. There is a destructive interference between the diagrams, and thus the cross section for large K_e turns out to be greater than the cross section when both K_γ and K_e are large. We notice that rather large values of K_γ and K_e are required to obtain the cross section around $\mathcal{O}(10^{2-3})$ fb with the eV order gravitino mass, while such large values are not favored by the stability of the SUSY breaking vacuum [15].

Since the $\tilde{\chi}_1^0 \to \gamma \tilde{G}^{(')}$ decay is isotropic, the photon distribution is given by purely kinematical effects of the decaying neutralino. Figure 3 shows normalized energy (left) and angular (right) distributions of the photon for the signal (5) as well as the SM background at $\sqrt{s} = 500$ GeV. The minimal cuts for the detection of photons

$$E_\gamma > 0.03\sqrt{s} = 15 \text{ GeV}, \quad |\eta_\gamma| < 2, \tag{6}$$

and the Z-peak cut to remove the SM $(Z \to \nu\bar{\nu})\gamma$ background

$$E_\gamma < \frac{s - m_Z^2}{2\sqrt{s}} - 5\Gamma_Z \sim 230 \text{ GeV}, \tag{7}$$

are imposed. The most significant background coming from the t-channel W-exchange process can be reduced by using polarized $e^\pm$ beams, while the distributions do not change so much both for signal and background; see more quantitative details in [7].

The energy distributions are flat, and the maximal and minimal energy are given by

$$E_\gamma^{\max,\min} = \frac{\sqrt{s}}{4}\hat{\beta}\left(1 + \frac{m_{\tilde{\chi}_1^0}^2 - m_{\tilde{G}'}^2}{s} \pm \beta\right), \tag{8}$$

where $\hat{\beta} = 1$ for $\tilde{\chi}_1^0 \to \gamma\tilde{G}$ and $(1 - \frac{m_{\tilde{G}'}^2}{m_{\tilde{\chi}}^2})$ for $\tilde{\chi}_1^0 \to \gamma\tilde{G}'$, and $\beta = \bar{\beta}(\frac{m_{\tilde{\chi}}^2}{s}, \frac{m_{\tilde{G}'}^2}{s})$ with $\bar{\beta}(a, b) = (1 + a^2 + b^2 - 2a - 2b - 2ab)^{1/2}$. The higher edge can determine the pseudo-goldstino mass when the $\tilde{\chi}_1^0 \to \gamma\tilde{G}'$ decay is significant.

On the other hand, the angular distributions are not sensitive to the pseudo-goldstino mass, and hence only the $m_{\tilde{G}'} = 0$ case is shown in Fig. 3 (right). Instead the distributions depend on the coupling factors K_γ and K_e. This is because that the distributions are determined by how much the s-channel and t, u-channel diagrams contribute. The selectron-exchange contribution can be enhanced by increasing K_e as well as $m_{\tilde{e}}$, which lead to the flatter distributions; see more details on the $m_{\tilde{e}}$ dependence in [7].

4   Summary

We extended our previous study on the mono-photon plus missing energy signal in the $\tilde{\chi}_1^0$-$\tilde{G}$ associated production at future linear colliders [7]. All the results presented here can be obtained numerically running `MadGraph5` [14] simulations adapted to the (pseudo)-goldstino scenario (building on [6]), having implemented the model using `FeynRules` [12,13]. Comparing with the multiple goldstino scenario [15], we showed that the energy and angular distributions of the photon can explore the SUSY masses as well as the SUSY breaking mechanism.

Before closing, we note that single-electron plus missing energy signals in $\tilde{e}$-$\tilde{G}$ associated productions at $e\gamma$ colliders were also studied in detail in Ref. [7].

Acknowledgments

Appendix A: Pseudo-goldstino interaction Lagrangian

We briefly present the relevant terms of the pseudo-goldstino interaction Lagrangian for our study both in the derivative and non-derivative forms, which were implemented into `FeynRules` [12] to obtain the `UFO` model file [13] for `MadGraph5` [14].

- In the derivative form:

$$
\begin{aligned}
\mathcal{L}_{\partial\tilde{G}'} = &\pm \frac{iK_e}{\sqrt{3}\,\overline{M}_{\mathrm{Pl}}\,m_{3/2}} \big[\partial_\mu\bar{\psi}_{\tilde{G}'}\gamma^\nu\gamma^\mu P_\pm \psi_e \, \partial_\nu\phi_{\tilde{e}_\pm}^* - \bar{\psi}_e P_\mp \gamma^\mu\gamma^\nu \partial_\mu\psi_{\tilde{G}'} \, \partial_\nu\phi_{\tilde{e}_\pm} \big] \\
&- \frac{iK_\gamma C_{\gamma\tilde{\chi}_i}}{4\sqrt{6}\,\overline{M}_{\mathrm{Pl}}\,m_{3/2}} \partial_\mu\bar{\psi}_{\tilde{G}'}[\gamma^\nu, \gamma^\rho]\gamma^\mu\psi_{\tilde{\chi}_i^0}(\partial_\nu A_\rho - \partial_\rho A_\nu) \\
&- \frac{iK_{Z_T} C_{Z_T\tilde{\chi}_i}}{4\sqrt{6}\,\overline{M}_{\mathrm{Pl}}\,m_{3/2}} \partial_\mu\bar{\psi}_{\tilde{G}'}[\gamma^\nu, \gamma^\rho]\gamma^\mu\psi_{\tilde{\chi}_i^0}(\partial_\nu Z_\rho - \partial_\rho Z_\nu) \\
&- \frac{2m_Z K_{Z_L} C_{Z_L\tilde{\chi}_i}}{\sqrt{6}\,\overline{M}_{\mathrm{Pl}}\,m_{3/2}} \partial_\mu\bar{\psi}_{\tilde{G}'}\psi_{\tilde{\chi}_i^0} Z^\mu,
\end{aligned} \tag{9}
$$

where the couplings related to the neutralino mixing defined by $X_i = U_{ij}\tilde{\chi}_j^0$ in the $X = (\tilde{B}, \tilde{W}^3, \tilde{H}_d^0, \tilde{H}_u^0)$ basis are

$$
\begin{aligned}
C_{\gamma\tilde{\chi}_i} &= U_{1i}\cos\theta_W + U_{2i}\sin\theta_W, \\
C_{Z_T\tilde{\chi}_i} &= -U_{1i}\sin\theta_W + U_{2i}\cos\theta_W, \\
C_{Z_L\tilde{\chi}_i} &= U_{3i}\cos\beta - U_{4i}\sin\beta,
\end{aligned}
\tag{10}
$$

with the ratio of the vacuum expectation value of the two Higgs doublets $\tan\beta$. K_e, K_γ, K_{Z_T} and K_{Z_L} are parameters characterizing the pseudo-goldstino couplings [15], and the $K = 1$ limit reduces (9) to that for the pure goldstino.

- In the non-derivative form:

$$
\begin{aligned}
\mathcal{L}_{\eth\tilde{G}'} = {}&\mp \frac{iK_e m_{\tilde{e}_\pm}^2}{\sqrt{3}\,\overline{M}_{\mathrm{Pl}}\,m_{3/2}} \left[\bar{\psi}_{\tilde{G}'} P_\pm \psi_e\, \phi_{\tilde{e}_\pm}^* - \bar{\psi}_e P_\mp \psi_{\tilde{G}'}\, \phi_{\tilde{e}_\pm} \right] \\
&- \frac{K_\gamma C_{\gamma\tilde{\chi}_i} m_{\tilde{\chi}_i^0}}{4\sqrt{6}\,\overline{M}_{\mathrm{Pl}}\,m_{3/2}} \bar{\psi}_{\tilde{G}'}[\gamma^\mu,\gamma^\nu]\psi_{\tilde{\chi}_i^0}(\partial_\mu A_\nu - \partial_\nu A_\mu) \\
&- \frac{K_{Z_T} C_{Z_T\tilde{\chi}_i} m_{\tilde{\chi}_i^0} + K_{Z_L} C_{Z_L\tilde{\chi}_i} m_Z}{4\sqrt{6}\,\overline{M}_{\mathrm{Pl}}\,m_{3/2}} \bar{\psi}_{\tilde{G}'}[\gamma^\mu,\gamma^\nu]\psi_{\tilde{\chi}_i^0}(\partial_\mu Z_\nu - \partial_\nu Z_\mu) \\
&- \frac{im_Z(K_{Z_T} C_{Z_T\tilde{\chi}_i} m_Z + K_{Z_L} C_{Z_L\tilde{\chi}_i} m_{\tilde{\chi}_i^0})}{\sqrt{6}\,\overline{M}_{\mathrm{Pl}}\,m_{3/2}} \bar{\psi}_{\tilde{G}'}\gamma^\mu\psi_{\tilde{\chi}_i^0} Z_\mu.
\end{aligned}
\tag{11}
$$

References

[1] J. Abdallah *et al.* [DELPHI Collaboration], Eur. Phys. J. C **38** (2005) 395.

[2] P. Fayet, Phys. Lett. B **175** (1986) 471.

[3] D. A. Dicus, S. Nandi and J. Woodside, Phys. Lett. B **258** (1991) 231.

[4] J. L. Lopez, D. V. Nanopoulos and A. Zichichi, Phys. Rev. Lett. **77**, 5168 (1996); Phys. Rev. D **55**, 5813 (1997).

[5] K. Hagiwara, K. Mawatari and Y. Takaesu, Eur. Phys. J. C **71** (2011) 1529.

[6] K. Mawatari and Y. Takaesu, Eur. Phys. J. C **71** (2011) 1640.

[7] K. Mawatari, B. Oexl and Y. Takaesu, Eur. Phys. J. C **71** (2011) 1783.

[8] J. R. Ellis, K. Enqvist and D. V. Nanopoulos, Phys. Lett. B **147** (1984) 99; ibid. **151** (1985) 357.

[9] J. L. Lopez, D. V. Nanopoulos and A. Zichichi, Phys. Rev. D **49** (1994) 343; Int. J. Mod. Phys. A **10** (1995) 4241.

[10] T. Gherghetta and A. Pomarol, Nucl. Phys. B **586** (2000) 141; ibid. **602** (2001) 3.

[11] See, e.g., G. F. Giudice and R. Rattazzi, Phys. Rept. **322** (1999) 419.

[12] N. D. Christensen and C. Duhr, Comput. Phys. Commun. **180** (2009) 1614; C. Duhr and B. Fuks, Comput. Phys. Commun. **182**, 2404 (2011).

[13] C. Degrande, C. Duhr, B. Fuks, D. Grellscheid, O. Mattelaer and T. Reiter, arXiv:1108.2040 [hep-ph].

[14] J. Alwall, M. Herquet, F. Maltoni, O. Mattelaer and T. Stelzer, JHEP **1106** (2011) 128.

[15] R. Argurio, K. De Causmaecker, G. Ferretti, A. Mariotti, K. Mawatari and Y. Takaesu, arXiv:1112.5058 [hep-ph].

[16] C. Cheung, Y. Nomura and J. Thaler, JHEP **1003** (2010) 073; N. Craig, J. March-Russell and M. McCullough, JHEP **1010** (2010) 095.

[17] R. Argurio, Z. Komargodski and A. Mariotti, Phys. Rev. Lett. **107** (2011) 061601.